Random Dopant-Induced Variability in Si-InAs Nanowire Tunnel FETs: A Quantum Transport Simulation Study

Hamilton Carrillo-Nuñez, Jaehyun Lee, Salim Berrada, Cristina Medina-Bailón, Fikru Adamu-Lema, Mathieu Luisier, Asen Asenov, *Fellow, IEEE*, and Vihar P. Georgiev, *Member, IEEE*

***Abstract*—In this letter, we report a quantum transport simulation study of the impact of random discrete dopants (RDDs) on Si-InAs nanowire p-type Tunnel FETs. The band-to-band tunneling is simulated using the non-equilibrium Green's function formalism in effective mass approximation, implementing a two-band model of the imaginary dispersion. We have found that RDDs induce strong variability not only in the OFF-state but also in the ON-state current of the TFETs. Contrary to the nearly normal distribution of the RDD-induced ON-current variations in conventional CMOS transistors, the TFET's ON-currents variations are described by a logarithmic distribution. The distributions of other figures of merit (FoM) such as threshold voltage and subthreshold swing are also reported. The variability in the FoM is analyzed by studying the correlation between the number and the position of the dopants.**

***Index Terms*—Randomly discrete dopants, variability, Si-InAs nanowire FETs, NEGF, quantum transport.**

I. Introduction

Band-to-band tunneling (BTBT) field-effect transistors (TFETs) have been extensively studied over the last decade as potential candidates for low-power electronic devices [1]. In theory, thanks to the BTBT, the TFET could achieve a sub-thermal (less than 60 mV/decade) subthreshold swing (SS).

Hetero-TFETs made of III-V semiconductors on Si were proposed to reduce the BTBT barrier and consequently to increase the ON-current (I_{ON}) [2], [3]. Despite the substantial I_{ON} improvement, there are still leakage mechanisms limiting the hetero-TFET performance, such as trap-assisted tunneling [4] arising from defect states at the heterojunction interface, or electronic states in the forbidden energy gap region occurring due to the Random Discrete Dopants (RDDs). Although the effect of RDD in metal-oxide-semiconductor FETs (MOSFETs) [5], [6] and junctionless FETs [7], [8] has been widely studied, there is still a lack of research and understanding of their impact on nanowire TFETs [9].

In this letter, we report results of a thorough statistical analysis of the RDD-induced variability in a Si-InAs nanowire TFET illustrated in Fig. 1. The letter is organized as follows. The simulation methodology for this study is presented in Section II. Then, the main findings from the statistical simulations are reported in Section III, and finally the conclusions are drawn in Section IV.

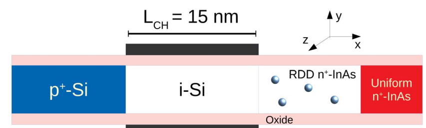

Fig. 1. Sketch of the Si-InAs nanowire TFET along the transport direction considered in this work. The intrinsic Si region is covered by the gate. As the tunneling is mainly happening at the InAs and i-Si interface, RDD is only considered in the InAs region. The nanowire diameter is 3.5 nm and the effective oxide thickness is 0.46 nm.

II. Simulation Methodology

Fig. 1 shows a sketch of the Si-InAs nanowire p-type TFET considered in this work with an ideal and abrupt interface. The gate is 15 nm long, covering all-around the intrinsic Si nanowire region, and the nanowire diameter is $2R = 3.5$ nm. The transport occurs along the $\langle 111 \rangle$ crystallography direction. The p^+-type (Si) drain and n^+-type (InAs) source are highly doped with $N_A = 2 \times 10^{20}\mathrm{cm}^{-3}$ and $N_D = 10^{19}\mathrm{cm}^{-3}$, respectively. The effective oxide thickness is 0.46 nm and the applied source-to-drain bias (V_{DS}) is fixed to -1.0 V. The devices are simulated at room temperature.

In Si-InAs TFETs, the BTBT is mainly direct and no phonon-assisted tunneling occurs [10]. The inclusion of the phonon scattering, although would lead to more accurate predictions, it was reported to change negligibly the ON-state current, whereas it slightly increases the OFF-state current of TFETs [11]. Therefore, electron-phonon interactions should not influence the conclusions of this study.

The quantum transport problem for electrons and holes is independently solved within the one-band effective mass approximation (EMA), by using the non-equilibrium Green's function (NEGF) technique in mode-space representation and coupled self consistently to the Poisson equation. The total

Manuscript received July 11, 2018; revised July 19, 2018; accepted July 21, 2018. Date of publication July 25, 2018; date of current version August 23, 2018. This work was supported by the U.K. EPSRC under Project EP/P009972/1. The review of this letter was arranged by Editor V. Moroz. *(Corresponding author: Hamilton Carrillo-Nuñez.)*

H. Carrillo-Nuñez, J. Lee, S. Berrada, C. Medina-Bailón, F. Adamu-Lema, A. Asenov, and V. P. Georgiev are with the School of Engineering, University of Glasgow, Glasgow G12 8LT, U.K. (e-mail: hacarrillo@gmail.com).

M. Luisier is with the Integrated Systems Laboratory, ETH Zürich, 8092 Zürich, Switzerland.

Color versions of one or more of the figures in this letter are available online at http://ieeexplore.ieee.org.

Digital Object Identifier 10.1109/LED.2018.2859586

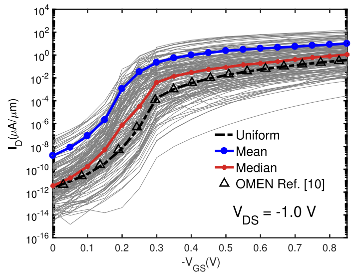

Fig. 2. $I_D - V_{GS}$ characteristics of the 150 Si-InAs nanowire TFETs with randomly distributed dopants (gray curves). The statistical mean and median are also plotted. The Si-InAs nanowire TFET with a uniform doping profile is shown as reference. The current is normalized by $2\pi R$.

carrier density determines the new potential. Once the convergence is reached, the valence and conduction bands are bridged through the two-band model of the imaginary dispersion proposed by Flietner [12].

The Flietner model has already been proven to reproduce accurately the full-band and atomistic results of different bulk-diodes [13] and Si-InAs nanowires TFETs [10], as long as the correct potential and proper material parameters are provided. For the latter, the WKB approximation is employed. Whereas for the former, the diode current is computed using the NEGF formalism. Here, we implement and adapt the Flietner model to calculate the BTBT current in nanowire TFETs by means of NEGF. The electron and hole effective masses are extracted from the full-band structure computed with the atomistic tool OMEN [14], based on the $sp^3d^5s^*$ tight-binding model. For the Si nanowire the electron and valence masses are $m_c = (0.45m_0, 0.27m_0, 0.27m_0)$ and $m_v = (0.11m_0, 1.44m_0, 1.44m_0)$, respectively, with rest mass m_0. In case of InAs, $m_c = (0.072m_0, 0.22m_0, 0.22m_0)$ and $m_v = (0.072m_0, 0.26m_0, 0.26m_0)$. The valence (conduction) band offset is also extracted from the full-band simulations: $\Delta E_v = 0.18$ eV ($\Delta E_c = 0.63$ eV). Band non-parabolicity, with $\alpha_{NP} = 1.4$ eV^{-1}, is also taken into account for the conduction band when solving the transport problem in the InAs region.

We benchmarked our in-house quantum transport tool, called NESS, against OMEN. The source and drain regions of the Si-InAs nanowire TFET in Fig. 1 are assumed to be uniformly doped. The results are in agreement with the full-band transport simulations [10], as observed in Fig. 2. We believe that the good agreement with the atomistic simulations is due to a well-defined parabolic curvature of the highest subbands observed in the Si valence band. This cannot be generalized because it might not be the case for other materials or crystallographic directions.

In the Si-InAs heterojunction configuration, BTBT occurs between the n$^+$-doped InAs and the i-Si regions. RDD is, therefore, only considered in the InAs part of the device. The RDD region is 20 nm long, as shown in Fig. 1, preceded by an uniform doped region required for numerical stability. The number of dopants in each of the TFETs is randomly chosen from a Poisson distribution, with the mean determined by the doping concentration multiplied by the volume of the RDD region. The dopants are then randomly placed using a probability rejection technique. For the statistical study shown below, an ensemble of 150 Si-InAs nanowire TFETs with RDD is simulated.

TABLE I
STATISTICAL SUMMARY OF FoM FOR THE ENSEMBLE OF THE 150 Si-InAs NANOWRIE TFETs WITH RDD SIMULATED IN THIS WORK

	$\log_{10}(I_{ON})$	$\log_{10}(I_{OFF})$	V_{TH} (V)	SS (mV/dec)
FoM Mean	-0.045	-11.35	0.49	34
σFoM	1.10	1.65	0.07	13
Min. Value	-3.6	-14.6	0.31	15
Max. Value	2.2	-7.2	0.72	81

III. RESULTS AND DISCUSSION

Fig. 2 shows the $I_D - V_{GS}$ characteristics for an ensemble of 150 Si-InAs nanowire TFETs. The currents are normalized by the nanowire cross section perimeter ($2\pi R$). The simulated OFF-currents (I_{OFF}), defined at $V_{GS} = 0$ V, range from $2.7 \times 10^{-15} \mu A/\mu m$ to $6.6 \times 10^{-8} \mu A/\mu m$, showing approximately seven orders of magnitude difference. The variability in the ON-state current ($V_{GS} = -0.85$ V) is comparable with I_{ON} varying between $2.7 \times 10^{-4} \mu A/\mu m$ and $I_{ON} = 105\ \mu A/\mu m$. The statistical summary of the most important Figures of Merit (FoM) is provided in Table I. The minimum and maximum value for each FoM are given together with their standard deviation (σFoM). For instance, the simulated mean threshold voltage (V_{TH}) is found to be 0.49 V with $\sigma V_{TH} = 0.07$ V. The V_{TH} is computed by using a threshold current criterion of $10^{-6} \mu A/\mu m$.

The mean and median $I_D - V_{GS}$ characteristics of the 150 Si-InAs nanowire TFETs are also reported in Fig. 2. The $I_D - V_{GS}$ characteristic corresponding to the TFET with uniform doping profile is added as a reference. The mean and median I_{ON} are 28× and 3× the uniform $I_{ON} \approx 0.4 \mu A/\mu m$, respectively. In the low bias regime, one can observe that the mean I_{OFF} is much higher not only if compared to the uniform I_{OFF}, but also if compared to the median I_{OFF}. This is typical for parameters with logarithmic-normal distribution, like the leakage current in conventional MOSFETs. However, the SS of all three $I_D - V_{GS}$ characteristics is comparable. The SS for the uniform TFET is 48 mV/dec. The mean and median SS values are 34 mV/dec and 35 mV/dec, respectively. The SS is computed as an average of the point SS at each gate bias, $SS = \sum_j SS(V_{GS,j}) \Delta V_{GS,j} / \sum_j \Delta V_{GS,j}$, within a range of $\sum_j \Delta V_{GS,j} = 250$ mV, where the current approximately varies seven orders of magnitude.

In MOSFETs with RDD-induced variability, the mean and median $I_D - V_{GS}$ characteristics lead to the similar current in the ON-state, with close to normal statistical distribution. However, OFF-currents follow a logarithmic-normal distribution, leading to big differences between the mean and the median currents. Here, as shown in Fig. 2, the mean and median ON-state currents of TFETs are significantly different. This is an interesting and important result. Contrary to MOSFETs, we have found that the ON-state currents of TFETs with RDD-induced variability are described by a logarithmic-normal distribution. This can be understood by keeping in mind that the ON-state in a TFET is still controlled by the BTBT barrier length. In the presence of RDD, the barrier width and height, as well as the FoM, depends on the number of dopants and their position, as indicated in Fig. 3 and Fig. 5. In the Si-InAs nanowire TFET illustrated in Fig. 3(a), there is only one dopant, whereas in the device illustrated in Fig. 3(b) there are five dopants. Their specific positions can be seen in the insets in Fig. 3.

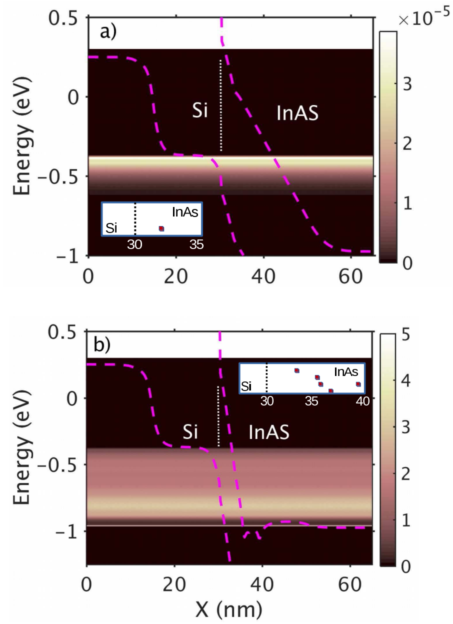

Fig. 3. Simulated ON-state current-spectra of the Si-InAs nanowire TFETs with (a) one and (b) five dopants. The units are μA/eV. The insets show their position in each TFET. The pink dashed-lines denote the highest valence and the lowest conduction subbands. The vertical white dashed-line indicates the Si-InAs interface.

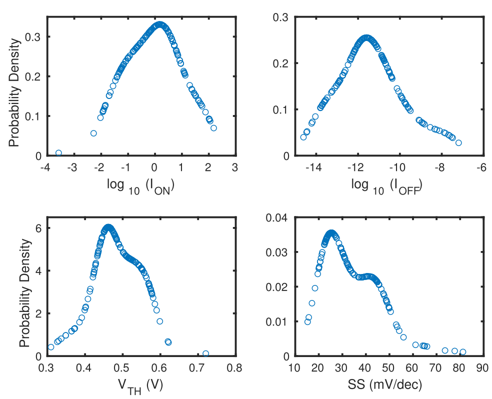

Fig. 4. Probability density functions of the most important Figures of Merit obtained from the simulation of the ensemble of 150 Si-InAs nanowrie TFETs shown in Fig. 2.

In comparison with other key sources of variability such as trap-states, where the main impact occurs on the OFF-state of the TFET [15], or surface roughness which reduces the BTBT current while presenting less variability [11], the RDD-induced variability significantly impact the device characteristics.

Fig. 4 shows the probability density functions (PDFs) of the following FoM: $\log_{10}(I_{ON})$, $\log_{10}(I_{OFF})$, V_{TH}, and SS. Notice that a logarithmic distribution for the ON- and OFF-currents is used to calculate their PDF. The mean values of $\log_{10}(I_{ON})$ and $\log_{10}(I_{OFF})$ are located approximately at -0.045 dec and -11.35 dec, respectively, corresponding to $I_{ON} \approx 1\ \mu A/\mu m$ and $I_{OFF} \approx 4.5 \times 10^{-12}\ \mu A/\mu m$, being in agreement with the median values shown in Fig. 2.

RDDs also have a strong impact on the V_{TH} and SS. As seen in Fig. 4, the PDF reveals a large variation of the V_{TH}. The difference between the lowest and highest V_{TH} in the simulated ensemble of 150 transistors is 0.4 V. For SS, in the best case scenario, the lowest value is 15 mV/dec. The worst case TFET has the SS of 81 mV/dec. Note that the PDFs of the V_{TH} and SS are qualitatively alike. They both show a bi-modal Gaussian-like behavior. The mean values are at 0.46 V and 0.53 V for V_{TH}, and 24.8 and 42.1 for SS.

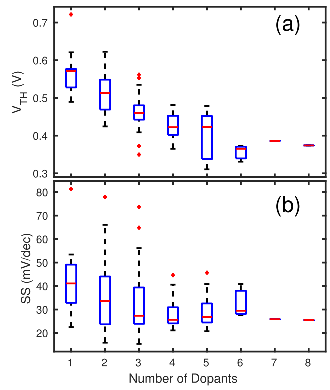

Fig. 5. Statistical analysis of (a) the threshold voltage and (b) subthreshold swing as a function of the number of dopants.

The presence of two headed Gaussian-like PDFs distribution can be understood by inspecting Fig. 5, where the statistical analysis of the FoM V_{TH} and SS of the 150 TFETs are grouped according to the number of dopants (n_D) in each of the devices. The red horizontal line indicates the mean value for each group of TFETs. From Fig. 5, for instance, one can observe that there are only two devices with $n_D = 7$ and $n_D = 8$. The group with $n_D = 2$ corresponds to the number of dopants that can exist in the RDD volume to satisfy the mean doping concentration. In the two headed Gaussian-like PDFs distribution of V_{TH} and SS, the first Gaussian function comes from the contribution of TFETs with $n_D > 2$. TFETs with few dopants ($n_D \leq 2$) dominate for higher V_{TH} and SS, giving rise to the second Gaussian-like region in the total PDFs.

IV. Conclusion

A statistical analysis of RDD variability in Si-InAs nanowire p-type TFETs has been performed. A statistical sample of 150 microscopically different transistors has been simulated. The impact of RDD on the key FoM has been found to be very strong. For instance, in contrast to regular MOSFETs, ON-currents of TFET showed to follow a logarithmic-normal distribution. We have also computed the probability density functions (PDFs) for each FoM. It has been found that the PDFs corresponding to the V_{TH} and SS have a bimodal Gaussian distribution. Such behavior is explained by correlating V_{TH} and SS with the number of dopants.

For the purpose of this research we have developed an in-house quantum transport module in the Glasgow nano-simulation environment NESS, based on the non-equilibrium Green's function formalism in the effective mass approximation, and on the Flietner model for the imaginary bandstructure dispersion. It has shown great accuracy when comparing with the state-of-the-art OMEN simulator, at much less computational cost.

References

[1] A. M. Ionescu and H. Riel, "Tunnel field-effect transistors as energy-efficient electronic switches," *Nature*, vol. 479, no. 7373, pp. 329–337, 2011, doi: 10.1038/nature10679.

[2] M. T. Björk, H. Schmid, C. D. Bessire, K. E. Moselund, H. Ghoneim, S. Karg, E. Lörtscher, and H. Riel, "Si–InAs heterojunction Esaki tunnel diodes with high current densities," *Appl. Phys. Lett.*, vol. 97, no. 16, p. 163501, 2010, doi: 10.1063/1.3499365.

[3] H. Riel, K. E. Moselund, C. Bessire, M. T. Björk, A. Schenk, H. Ghoneim, and H. Schmid, "InAs-Si heterojunction nanowire tunnel diodes and tunnel FETs," in *IEDM Tech. Dig.*, San Francisco, CA, USA, Dec. 2012, pp. 16.6.1–16.6.4, doi: 10.1109/IEDM.2012.6479056.

[4] S. Sant, K. Moselund, D. Cutaia, H. Schmid, M. Borg, H. Riel, and A. Schenk, "Lateral InAs/Si p-type tunnel FETs integrated on Si—Part 2: Simulation study of the impact of interface traps," *IEEE Trans. Electron Devices*, vol. 63, no. 11, pp. 4240–4247, Nov. 2016, doi: 10.1109/TED.2016.2612484.

[5] A. Asenov, "Simulation of statistical variability in nano MOSFETs," in *Proc. IEEE Symp. VLSI Technol.*, Jun. 2007, pp. 86–87, doi: 10.1109/VLSIT.2007.4339737.

[6] A. R. Brown, J. R. Watling, G. Roy, C. Riddet, C. L. Alexander, U. Kovac, A. Martinez, and A. Asenov, "Use of density gradient quantum corrections in the simulation of statistical variability in MOSFETs," *J. Comput. Electron.*, vol. 9, nos. 3–4, pp. 187–196, Dec. 2010, doi: 10.1007/s10825-010-0314-y.

[7] M. Aldegunde, A. Martinez, and J. R. Barker, "Study of discrete doping-induced variability in junctionless nanowire MOSFETs using dissipative quantum transport simulations," *IEEE Electron Device Lett.*, vol. 33, no. 2, pp. 194–196, Feb. 2012, doi: 10.1109/LED.2011.2177634.

[8] G. Leung and C. O. Chui, "Variability impact of random dopant fluctuation on nanoscale junctionless FinFETs," *IEEE Electron Device Lett.*, vol. 33, no. 6, pp. 767–769, Jun. 2012, doi: 10.1109/LED.2012.2191931.

[9] S. S. Sylvia, K. M. M. Habib, M. A. Khayer, K. Alam, M. Neupane, and R. K. Lake, "Effect of random, discrete source dopant distributions on nanowire tunnel FETs," *IEEE Trans. Electron Devices*, vol. 61, no. 6, pp. 2208–2214, Jun. 2014, doi: 10.1109/TED.2014.2318521.

[10] H. Carrillo-Nuñez, M. Luisier, and A. Schenk, "Analysis of InAs-Si heterojunction nanowire tunnel FETs: Extreme confinement vs. bulk," *Solid-State Electron.*, vol. 113, pp. 61–63, Nov. 2015, doi: 10.1016/j.sse.2015.05.019.

[11] H. Carrillo-Nuñez, R. Rhyner, M. Luisier, and A. Schenk, "Effect of surface roughness and phonon scattering on extremely narrow InAs-Si Nanowire TFETs," in *Proc. 46th Eur. Solid-State Device Res. Conf. (ESSDERC)*, Sep. 2016, pp. 188–191.

[12] H. Flietner, "The $E(k)$ relation for a two-band scheme of semiconductors and the application to the metal-semiconductor contact," *Phys. Status Solidi B*, vol. 54, no. 1, pp. 201–208, 1972.

[13] H. Carrillo-Nuñez, A. Ziegler, M. Luisier, and A. Schenk, "Modeling direct band-to-band tunneling: From bulk to quantum-confined semiconductor devices," *J. Appl. Phys.*, vol. 117, no. 23, p. 234501, Jun. 2015, doi: 10.1063/1.4922427.

[14] M. Luisier, A. Schenk, W. Fichtner, and G. Klimeck, "Atomistic simulation of nanowires in the $sp^3d^5s^*$ tight-binding formalism: From boundary conditions to strain calculations," *Phys. Rev. B, Condens. Matter*, vol. 74, no. 20, p. 205323, 2006, doi: 10.1103/PhysRevB.74.205323.

[15] D. Esseni and M. G. Pala, "Interface traps in InAs nanowire tunnel FETs and MOSFETs—Part II: Comparative analysis and trap-induced variability," *IEEE Trans. Electron Devices*, vol. 60, no. 9, pp. 2802–2807, Sep. 2013.